International Journal of Thermal Sciences 48 (2009) 1517–1522

Contents lists available at ScienceDirect

International Journal of Thermal Sciences

www.elsevier.com/locate/ijts

A modified truncation error-based adaptive time-step control strategy for fully- and semi-implicit simulation of isothermal solidification processes

Hsiun-Chang Peng, Long-Sun Chao *

Department of Engineering Science, National Cheng Kung University, Tainan City 701, Taiwan, ROC

ARTICLE INFO

Article history:
Received 29 February 2008
Received in revised form 5 October 2008
Accepted 18 December 2008
Available online 22 January 2009

Keywords:
Solidification
Adaptive time step
Finite difference
Truncation error

ABSTRACT

When analyzing the transient characteristics of solidification processes, choosing appropriately-sized time steps is difficult. Accordingly, the current study develops a modified local time truncation error (LTE)-based strategy designed to adaptively adjust the size of the time step during the simulated solidification procedure in such a way that the time steps can be adapted in accordance with the local variations in latent heat released during phase change or the effects of pure conduction in a single solid or liquid phase. In the approach presented in this work, the LTE-based time-step evaluation procedure is applied not only after a convergent temperature field is obtained at each time step, but also during the nonlinear iterations performed at each time step whenever a convergence problem is encountered. The computational accuracy and efficiency of the proposed method are demonstrated via the simulation of the one-dimensional and two-dimensional solidification problems and compared with those of other adaptive time step and the uniform time step methods. Furthermore, the performance of these approaches has also been demonstrated using fully-implicit and semi-implicit schemes.

1. Introduction

Solidification is a transient, discontinuous phase change process in which latent heat is released during the transformation from a liquid to a solid state and a reduction in the enthalpy of the liquid or the solid occurs as a result of cooling [1]. In the various mathematical models proposed to solve the solidification problem, fixed grid methods are commonly used, including the apparent heat capacity method, the enthalpy method, the source term method, the temperature recovery method, etc. However, when analyzing the transient characteristics of solidification processes with these methods, as described in [2–9], choosing appropriately-sized time steps for the applied time discretization technique is difficult. Normally, large time steps result in high truncation errors and therefore cause the simulations to miss the local effects of latent heat release, whilst smaller time steps enhance the accuracy of the numerical solutions, but inevitably increase the time and expense of the simulations. Accordingly, the objective of the current study is to develop an adaptive time-step control strategy to improve both the numerical accuracy and the computational efficiency when applied to the solution of solidification problems.

Although the literature contains many theoretical discussions of adaptive time step methods, the specific problem of modeling solidification processes has received relatively little attention. A variable time step (VTS) method, in which the spatial meshes were assigned an equal length and the time step was specified in such a way that the phase boundary moved through exactly one spatial mesh during each time step interval, was proposed by Douglas and Gallie [11] and was later modified by Goodling and Khader [12] and Gupta and Kumar [13,14]. These studies focused primarily on one-dimensional phase change problems and treated the energy balance between phases numerically using the Stefan condition. Ouyang and Tamma [15] developed an adaptive time stepping strategy based on a process of *a posteriori* error estimation for the simulation of solidification processes using a finite element method (FEM). The *a posteriori* estimator utilized a simple algorithm to determine the time step size when simulating one- or two-dimensional phase change problems.

Gresho, Lee and Sani (GLS) [16] developed a predictor–corrector strategy based on the second-order-accurate implicit trapezoid rule (TR) and the explicit Adams–Bashforth (AB) formula to vary the size of the time step adaptively in accordance with the estimated value of the local (i.e. single-step) time truncation error (LTE). FIDAP [17], a commercial FEM package marketed by Fluent Inc., applies the GLS predictor–corrector strategy to simulate the velocity and temperature fields in a variety of applications. However, as noted both in [17] and in the Finite Difference Method (FDM) study presented in [18], the time steps predicted by the GLS strategy based upon the apparent heat capacity method tend to be rather coarse and are therefore unsuited to the modeling of solidification processes since the simulations tend to skip over the latent heat release event. Accordingly, the current study proposes a mod-

* Corresponding author.
E-mail address: lschao@mail.ncku.edu.tw (L.-S. Chao).

1290-0729/$ – see front matter
doi:10.1016/j.ijthermalsci.2008.12.016

Nomenclature

L	characteristic length	m	
ρ	density	$kg\,m^{-3}$	
x	distance in x-direction	m	
y	distance in y-direction	m	
T_f	fusion temperature	°C	
C	heat capacity	$J\,kg^{-1}\,°C^{-1}$	
h_{int}	interfacial heat transfer coefficient	$W\,m^{-2}\,°C$	
L_f	latent heat	$J\,kg^{-1}$	
$d(T)$	local time truncation error (LTE)	°C	
T_m	mold temperature	°C	
s	position of liquid–solid interface	m	
ε	pre-defined value		
T_p	pouring temperature	°C	
T	temperature	°C	
ΔT	temperature difference of artificial mushy zone	°C	
ΔT_f	temperature difference in ΔT	°C	
k	thermal conductivity	$W\,m^{-1}\,°C^{-1}$	
α	thermal diffusivity	$m^2\,s^{-1}$	
t	time	s	
Δt	time step	s	

Subscripts and superscripts

app	apparent value
ext	extreme value
L	liquid phase
i	node number in x-direction
j	node number in y-direction
P	predictor function
S	solid phase
k	successive iteration level
n	time level
sel	time step selection
adj	time step adjustment

Dimensionless groups

X	dimensionless distance in x-direction
Y	dimensionless distance in y-direction
θ_f	dimensionless fusion temperature
θ_m	dimensionless mold temperature
S	dimensionless position of liquid–solid interface
θ_p	dimensionless pouring temperature
θ	dimensionless temperature
$\Delta\theta$	dimensionless temperature difference of artificial mushy zone
$\Delta\theta_f$	dimensionless temperature difference in $\Delta\theta$
τ	dimensionless time
$\Delta\tau$	dimensionless time step
β	inverse of Stefan number (Ste^{-1})
Ste	Stefan number

ified LTE technique in which the GLS predictor–corrector strategy is modified to enable the time steps to be adapted in accordance with the release tempo of the latent heat over the course of the solidification process. In the proposed approach, the time step for the next time level or the time step in the current time level (when a convergence problem is encountered) is computed using a modified LTE formulation based upon the values of an assumed extreme time step and an extreme LTE.

In solving the solidification problems, the latent heat release which occurs during phase change is modeled using the apparent heat capacity method [4]. The feasibilities of the modified LTE adaptive time-step scheme presented in this study is demonstrated via its application to several one- and two-dimensional phase change problems. The results obtained using the proposed scheme are compared with those generated using the GLS, CN (Crank–Nicolson) and BE (Backward Euler) adaptive methods, respectively, and the corresponding uniform time step methods.

2. Governing equation combined with apparent heat capacity

The energy equations for the solid and liquid phases are combined with the formulation of the apparent heat capacity method to model solidification processes with the latent heat released during phase change, and expressed in the form

$$\rho C_{app}\frac{\partial T}{\partial t} = \nabla \bullet (k\nabla T), \tag{1}$$

where C_{app} is the apparent heat capacity, which is given by

$$C_{app} = \begin{cases} C_L, & T > T_f + \Delta T, \\ \dfrac{1}{2}\left(\dfrac{L_f}{\Delta T} + C_L + C_S\right) & T_f - \Delta T \leqslant T \leqslant T_f + \Delta T, \\ C_S, & T < T_f - \Delta T, \end{cases} \tag{2}$$

where subscripts S and L denote the solid and liquid regions, respectively, C is the heat capacity, T_f the fusion temperature, and ΔT the artificial temperature difference. Since the solidification problems considered in this study are nonlinear, the iteration method [19] for the implicit computation is adopted to compute the apparent heat capacity C_{app} of the apparent heat capacity method.

3. GLS and proposed adaptive time-step strategies

In the current study, the modified LTE technique modifies the LTE estimate of the conventional GLS predictor and corrector strategy. During the nonlinear iterations performed at each current time level, the modified LTE technique is used to adjust the current time step Δt_n at $(k+1)$th iteration whenever the value of k is larger than a predefined number. Having obtained a convergent temperature solution at each time level, the similar modified LTE technique is then used to select an appropriate time step Δt_{n+1} for the next time level. Since the adjustment process of the current time step Δt_n during the nonlinear iterations is similar to the selection process of the next time step Δt_{n+1}, only the latter one is discussed in the following sections.

3.1. Predictor function and corrector function

As the GLS scheme, the time-step control scheme proposed in this study employs the explicit Adams–Bashforth (AB) formula as the predictor function and the implicit trapezoid rule (TR) as the corrector function. The AB formula has the form

$$\text{AB:}\quad T^P_{n+1} = T_n + \frac{\Delta t_n}{2}\left[\left(2 + \frac{\Delta t_n}{\Delta t_{n-1}}\right)\dot{T}_n - \frac{\Delta t_n}{\Delta t_{n-1}}\dot{T}_{n-1}\right]. \tag{3}$$

Since $\dot{T}_{n-1}$ is required, the AB formula cannot be applied until the second time step. Error estimation therefore commences only once the second time step has been completed. The TR corrector function is formulated as

$$\text{TR:}\quad T_{n+1} = T_n + \frac{\Delta t_n}{2}(\dot{T}_n + \dot{T}_{n+1}). \tag{4}$$

Being implicit, TR can be applied directly to Eq. (1) to obtain the final temperature.

3.2. LTE estimate in GLS scheme and modified LTE estimate

In the GLS scheme, the LTE estimation process commences by performing Taylor series analyses of the predictor (AB) and corrector (TR) formulations. The estimated errors between the numerical solutions and the analytical solutions $T_{ana}(t_{n+1})$ at time step t_{n+1} are given by

$$\text{AB:}\quad T^p_{n+1} - T_{ana}(t_{n+1}) = -\frac{1}{12}\left(2 + 3\frac{\Delta t_{n-1}}{\Delta t_n}\right)\Delta t_n^3 \dddot{T}_n, \tag{5}$$

$$\text{TR:}\quad T_{n+1} - T_{ana}(t_{n+1}) \equiv d(T_{n+1}) = \frac{\Delta t_n^3}{12}\dddot{T}_n, \tag{6}$$

where $d(T_{n+1})$ is the estimated LTE of the TR solution. Since T^p_{n+1} and T_{n+1} are available, Eqs. (5) and (6) can be used to eliminate the two unknowns, i.e. $T_{ana}(t_{n+1})$ and $\dddot{T}_n$, and hence the estimated LTE of the TR solution in the GLS scheme can be obtained as

$$d(T_{n+1}) = \frac{T_{n+1} - T^p_{n+1}}{3(1 + \frac{\Delta t_{n-1}}{\Delta t_n})}. \tag{7}$$

However, in the time-step control strategy employed in the current study, an appropriate time step is determined not on the basis of $d(T_{n+1})$, as in the conventional GLS strategy, but from an extreme value of LTE, designated as $d(T_{n+1})_{\text{ext}}$, derived on the assumption of an extreme time step Δt_{ext}, whose absolute value is much larger than that of Δt_{n-1}. From the corrector function given in Eq. (6), $d(T_{n+1})_{\text{ext}}$ can be written as

$$d(T_{n+1})_{\text{ext}} \equiv \frac{\Delta t_{\text{ext}}^3}{12}\dddot{T}_n. \tag{8}$$

Adopting this definition of $d(T_{n+1})_{\text{ext}}$, the term Δt_n in the denominator of Eq. (7) can be replaced by Δt_{ext}, and thus the ratio of Δt_{n-1} to Δt_{ext} approaches zero, causing the value of the LTE computed in Eq. (7) to converge to an extreme value. Accordingly, $d(T_{n+1})_{\text{ext}}$ can be expressed as

$$d(T_{n+1})_{\text{ext}} = \frac{T_{n+1} - T^p_{n+1}}{3}. \tag{9}$$

The LTE can then be estimated by combining Eqs. (6) and (8) to give

$$d(T_{n+1}) = d(T_{n+1})_{\text{ext}}\left(\frac{\Delta t_n}{\Delta t_{\text{ext}}}\right)^3. \tag{10}$$

In this study, Δt_{ext} is determined as a function of the local temperature, thus allowing the effective capture of the local variations which take place as a result of the latent heat released during phase change or the effects of pure conduction.

3.3. Novel technique for determining Δt_{ext}

The Taylor series of $\dot{T}_{n+1}$ with forward expansion can be written as

$$\dot{T}_{n+1} = \dot{T}_n + \ddot{T}_n\Delta t_n + \frac{1}{2}\dddot{T}_n\Delta t_n^2 + O\left(\Delta t_n^3\right). \tag{11}$$

To prevent the appearance of another previous time step, i.e. Δt_{n-2}, the third-order derivative $\dddot{T}_n$ in Eq. (11) is replaced by applying Eqs. (6) and (7). As a result, Eq. (11) can be written in the following semi-implicit predictor form:

$$\dot{T}^p_{n+1} = \dot{T}_n\left(1 + \frac{\Delta t_n}{\Delta t_{n-1}}\right) - \dot{T}_{n-1}\frac{\Delta t_n}{\Delta t_{n-1}} + \left(T_{n+1} - T^p_{n+1}\right)\frac{1}{\frac{1}{2}(\Delta t_n + \Delta t_{n-1})}. \tag{12}$$

The first and second terms on the right-hand side of Eq. (12) can be replaced by Eq. (3) and by assuming $\Delta t_n = \Delta t_{\text{ext}}$ and $\Delta t_{\text{ext}} \gg \Delta t_{n-1}$, Δt_{ext} can be expressed in terms of the temperature and cooling rate as follows:

$$\Delta t_{\text{ext}} = 2\left(\frac{T_{n+1} - T_n}{\dot{T}^p_{n+1} + \dot{T}_n}\right). \tag{13}$$

It is found that Eq. (13) is similar to the TR corrector function given in Eq. (4) and the corresponding LTE can be approximated by Eq. (8). In other words, the modified LTE given in Eq. (10) can be estimated via the error comparison of two TR formulae, i.e. Eqs. (4) and (13), respectively.

3.3.1. Initialization of Δt_{ext}

If much smaller change occurs in the local temperature during phase change or between the initial condition and the condition after the following time step(s), the denominator of Eq. (13), i.e. the sum of the cooling rates, is close to zero, and hence a numerical error easily results. Accordingly, in the proposed approach, the denominator term is assigned a small tolerance, which is sufficient to prevent a zero denominator without adversely affecting the quality of the numerical solutions.

3.3.2. Controlling the magnitude of Δt_{ext}

Due to its temporal singularity characteristic in space, latent heat release cannot easily be analyzed using a Taylor series approach without applying some form of correction. In the apparent heat capacity method, this singularity problem is resolved by imposing a piecewise continuity of the temperature drop $2\Delta T$ (see Eq. (2)) as the artificial mushy zone. However, a large time step may cause the temperature drop between T_n and T_{n+1} to exceed the value of $2\Delta T$, thereby violating the piecewise continuity condition and missing the effect of latent heat. As a result, a smaller value of the time step should be applied when modeling the phase change phenomenon in the solidification process. In the modified LTE time-step approach used in this study, this is achieved by applying a correction to Δt_{ext}. In the proposed approach, rather than calculating the difference between T_n and T_{n+1} in Eq. (13), its value is artificially corrected to a small constant value ΔT_f close to zero in each of the specified time steps in order to maintain the temporal piecewise continuity state set by the apparent heat capacity method.

3.4. Time step selection

As in the GLS scheme, the LTEs over the entire domain are used to predict the next time step size by applying the constraint that the (relative) norm of the errors at the next step should be equal to a small pre-defined value ε, i.e.

$$\Delta t_{n+1} = \Delta t_n\left(\frac{\varepsilon}{\|d(\mathrm{T}_{n+1})\|}\right)^{1/3}, \tag{14}$$

where ε corresponds to the value of $\|d(T_{n+2})\|$ and is set to 0.001 in accordance with the GLS recommendation [16]. $\|d(T_{n+1})\|$ is determined via the weighted RMS norm [16].

4. Results and discussion

This section commences by comparing the performances of the GLS, CN, BE and proposed adaptive time step methods in solving several one- and two-dimensional phase change problems. The performance of the four schemes is also compared with that generated using the corresponding uniform time step methods.

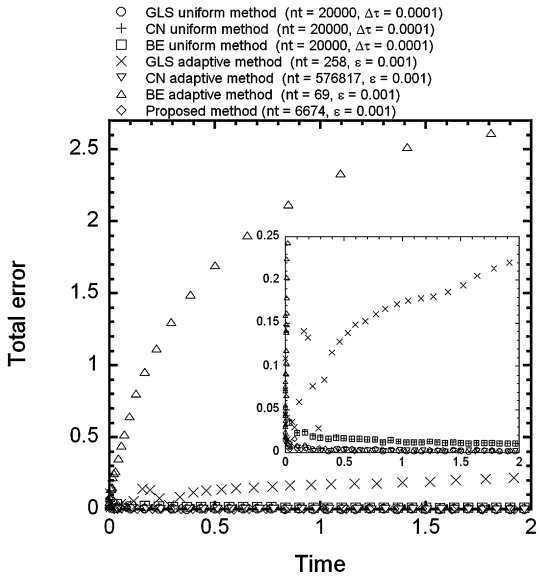

Fig. 1. One-dimensional phase change problem: total error histories of GLS, CN, BE and proposed adaptive and uniform time step methods.

4.1. One-dimensional phase change problem

The physical domain of this problem is a one-dimensional semi-infinite area. The initial pouring temperature T_p is assumed to be equal to the fusion temperature, T_f. When $t > 0$, $T = T_m$ (mold temperature) at $x = 0$. The position of the liquid–solid interface at any moment in time is indicated by $s(t)$. For convenience, the following dimensionless variables and parameters are introduced:

$$\theta = \frac{T - T_m}{T_f - T_m}, \qquad \tau = \frac{t\alpha_S}{L^2}, \qquad X = \frac{x}{L}, \qquad S = \frac{s}{L},$$

$$C^* = \frac{C_{\text{app}}}{C_S} \quad \text{and} \quad Ste = \frac{C_S(T_f - T_m)}{L_f},$$

where L is the characteristic length, L_f is the latent heat, and Ste is the Stefan number representing the inverse of dimensionless latent heat. α_S and C_S are the solid thermal diffusivity and heat capacity, respectively.

The analytical solution for this problem was originally derived by Stefan in [20]. In simulating this problem, it is assumed that the computing domain is from $X = 0$ to $X = 2$ and the space increment ΔX is 0.01. The mold temperature and fusion temperature thus become $\theta_m = 0$ and $\theta_f = 1$, respectively. The total calculation time is specified as $\tau = 2$ to ensure that $\theta(X = 2, \tau = 2) = 1$. In modeling the latent heat release process by the apparent heat capacity method, the temperature difference is $\Delta\theta = 0.001$ and $Ste = 1$. Note that because the pouring temperature θ_p is equal to the fusion temperature θ_f, only a half of $2\Delta\theta$ is required, where $\Delta\theta$ is the dimensionless ΔT. Based on the consideration of convergence, the $\Delta\theta_f$ terms used to calculate $\Delta\tau_{\text{ext}}$ in the $\Delta\tau_{n+1}$ selection process and the $\Delta\tau_n$ adjustment process are distinguished via the annotations $\Delta\theta_{f/\text{sel}}$ and $\Delta\theta_{f/\text{adj}}$, respectively and they are assigned by $\Delta\theta_{f/\text{sel}} = 10^{-7}$ and $\Delta\theta_{f/\text{adj}} = 10^{-15}$, respectively.

Fig. 1 compares the total error histories of the GLS, CN and BE uniform time step methods ($\Delta\tau = 0.0001$) with those of the GLS, CN, BE and proposed adaptive time step methods. Note that the total error is the square root of the total sum of the squared differences between the computational solution and the analytical solution over the entire domain. It is apparent that the results obtained using the proposed method are in very good agreement with those obtained using the GLS uniform time step method and the CN adaptive time step method. These schemes achieve a high degree

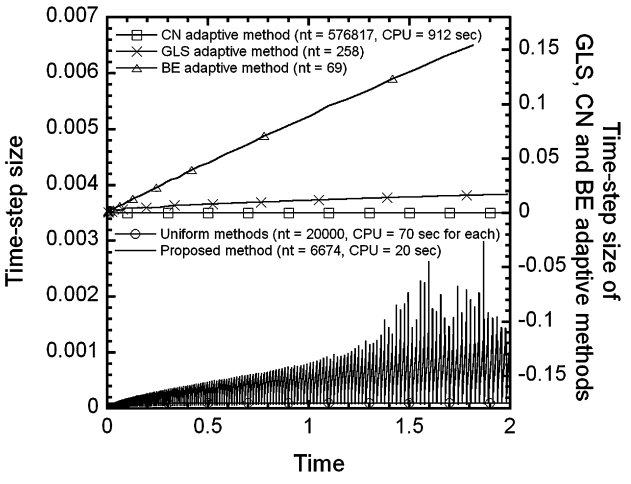

Fig. 2. One-dimensional phase change problem: time step size histories of GLS, CN, BE and proposed (left scale) adaptive and uniform time step methods.

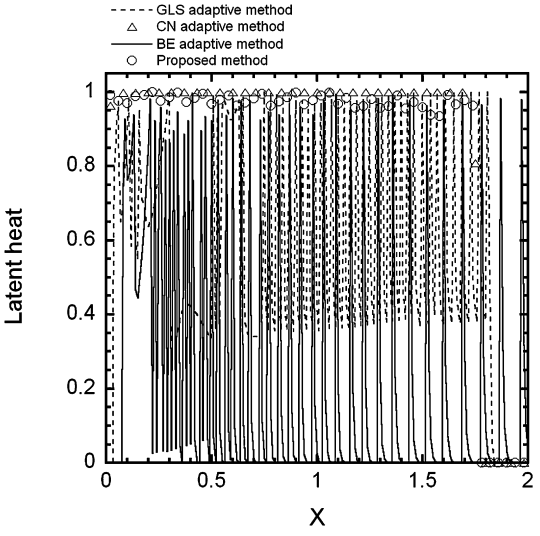

Fig. 3. One-dimensional phase change problem: latent heat release in space computed by GLS, CN, BE and proposed adaptive time step methods.

of numerical accuracy. However, the number of time steps required by the proposed method ($nt = 6674$) is significantly lower than that required by the GLS uniform time step method ($nt = 20000$) or the CN adaptive time step method ($nt = 576817$). In Fig. 2, it is observed that the time step size predicted by the GLS or BE adaptive time step methods increases approximately linearly over the course of the simulation. The time step size predicted by the CN adaptive time step method almost maintains at a small constant value. By contrast, those predicted by the proposed method oscillate strongly, albeit with a gradually increasing tendency. This phenomenon is the result of the accurate prediction of latent heat release. Furthermore, the figure shows that the proposed method has the smaller CPU time (performed by ASUS L7300 PC with a Pentium II 600 (MHz) CPU and 196 MB RAM).

Fig. 3 illustrates the latent heat release predictions of the GLS, CN, BE and proposed adaptive time step methods for all of the spatial nodes over the course of the simulation. The exact solution for the latent heat in this example is $1/Ste = 1$. The CN adaptive time step method can release the total amount of latent heat up to 99.9% of the exact value at $\tau = 2$ due to the nearly invariant small time steps. The total latent heat released by the proposed method reaches 97.5%. By contrast, 59.41% of the total latent heat is released by the GLS adaptive time step method and 26.37% by

the BE adaptive time step method. Consequently, the GLS and BE adaptive time step methods have the faster solidification rate and therefore the phase change position simulated by the GLS adaptive time step method reaches $X = 1.85$ at $\tau = 2$ rather than $X = 1.76$, as determined analytically, and the one simulated by the BE adaptive time step method exceeds $X = 2$. The phase change position for the proposed method reaches $X = 1.77$, which is much closer to the analytical one. Note that in this simulation, the computing domain of the BE adaptive time step method is from $X = 0$ to $X = 4$, which is enlarged corresponding to its faster solidification rate.

4.2. Two-dimensional phase change problem

An infinite corner region is assumed initially to be in a liquid state at a pouring temperature T_p higher than the melting temperature T_f. As time elapses, the boundary temperatures along $x = 0$ and $y = 0$, respectively, are either maintained at a constant mold temperature T_m or experience a convective effect with the ambient temperature T_{amb}. Both T_m and T_{amb} are lower than T_f. Note that the GLS, CN and BE uniform and adaptive time step methods are not considered in Section 4.2.1 (fixed temperature boundary condition) since they are known to suffer numerical instability [4,5] when applied to the two-dimensional problem with the fully-implicit scheme (FIS). Accordingly, in Section 4.2.2 (convective boundary condition), the semi-implicit scheme (SIS) is applied for the various time stepping methods. In the FIS scheme as applied in Section 4.1, the apparent heat capacity is iteratively calculated according to the temperature of current time step, whereas in the semi-implicit scheme (SIS), it is based on the temperature of previous time step and thus nonlinear iterations are not required.

4.2.1. Fixed temperature boundary condition

The dimensionless analytical solution and interface position for this 2-D phase change problem are given by Rathjen and Jiji in [21]. In the dimensionless physical model, the mold, fusion and pouring temperatures are specified as $\theta_m = -1$, $\theta_f = 0$ and $\theta_p = 0.3$, respectively. Furthermore, the computational domain is assumed to be in the shape of a square with sides of length $X = Y = 2$. In solving the problem using the proposed method implemented in the FIS scheme, the following parameter values are assigned: $\Delta X = \Delta Y = 10^{-2}$, $2\Delta\theta = 2 \times 10^{-2}$, $\Delta\theta_{f/\text{sel}} = 10^{-4}$ and $\Delta\theta_{f/\text{adj}} = 10^{-16}$.

Fig. 4 compares the exact and simulated solutions for the phase change position (i.e. the location of the liquid–solid interface) at $\tau = 0.25$ for the case of $\beta = 0.25$, where β is a non-dimensional parameter defined as $L_f/[C_S(T_f - T_m)]$, i.e. the inverse of the Stefan number. It can be seen that the simulated phase change interface is in good agreement with the exact solution. Analyzing the latent heat balance, the proposed scheme has 99.49% of the exact value (0.25). As shown in Fig. 5, this accurate latent heat balance performance results in an oscillating time-step history profile, similar to that observed in Section 4.1.

4.2.2. Convective boundary condition

The molten material was assumed to be pure aluminum and was poured into the mold at a temperature of $T_p = 680\,^\circ\text{C}$. The mold/metal interfacial heat transfer coefficient was assumed to be $h_{\text{int}} = 100\ \text{W/m}^2\,^\circ\text{C}$, the melting temperature was specified as $T_f = 660\,^\circ\text{C}$ and the ambient temperature was taken to be $T_{\text{amb}} = 25\,^\circ\text{C}$. The geometry in this problem is a 20×20 cm square with $\Delta x = \Delta y = 0.2$ cm. ΔT and ΔT_f in this example are specified as 0.1 and $10^{-6}\,^\circ\text{C}$, respectively. The exact latent heat is 408989 J/kg.

Fig. 6 shows the phase change locations following an elapsed time of 1600 sec as computed by the GLS, CN, BE and proposed adaptive methods, respectively, and the corresponding uniform

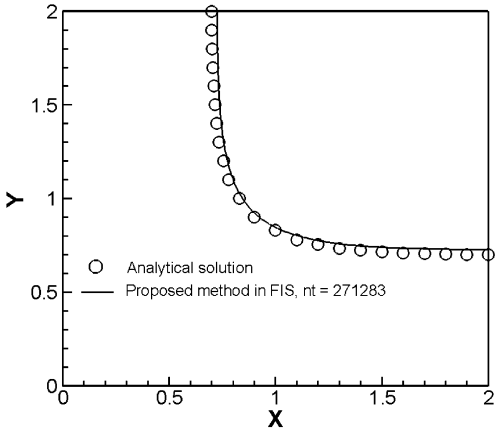

Fig. 4. Two-dimensional phase change problem with fixed temperature boundary condition: liquid–solid interface position computed by proposed method implemented in FIS scheme.

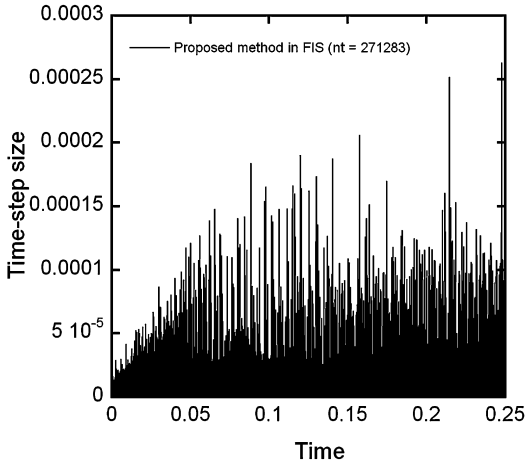

Fig. 5. Two-dimensional phase change problem with fixed temperature boundary condition: time step size history computed by proposed method implemented in FIS scheme.

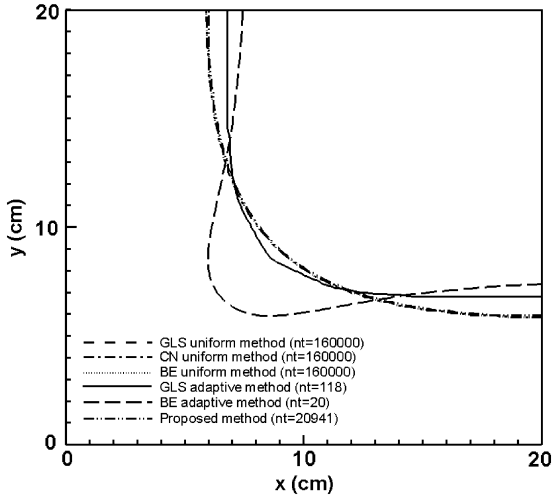

Fig. 6. Two-dimensional phase change problem with convective boundary condition: interfacial positions simulated by uniform time step methods and GLS, BE and proposed adaptive time step methods.

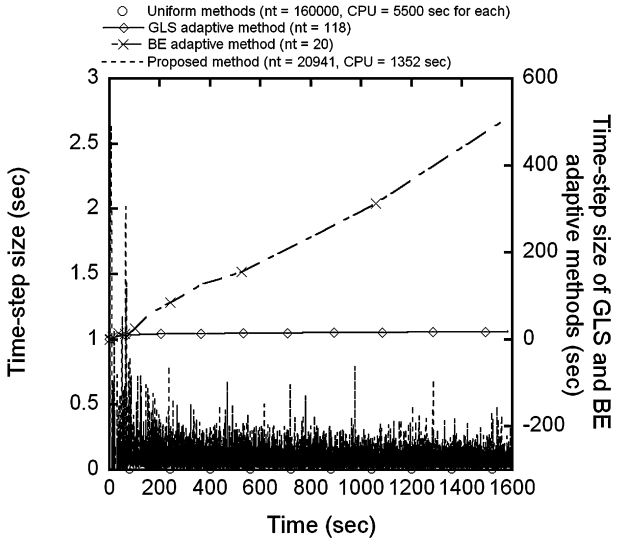

Fig. 7. Two-dimensional phase change problem with convective boundary conditions: time step histories computed by uniform time step methods and GLS, BE and proposed (left scale) adaptive time step methods.

time step methods. It can be seen that the simulated liquid–solid interface of the proposed method is in close agreement with those of the GLS, CN and BE uniform time step methods. Both the GLS and BE adaptive time step methods have the inconsistent solidification speed because they predict too large time steps to accurately detect the release of latent heat. As described in [10] and Section 4.1, the CN uniform time step scheme with a smaller time step can reach a comparable accuracy. However, the corresponding adaptive method presented in this example produces oscillated temperature phenomena over the entire computational domain due to improperly chosen time steps and therefore its erroneous result is not presented in the figure. It is found that the GLS, BE and proposed adaptive time step methods release approximately 50.62%, 12.91% and 97.82% of the exact total latent heat, respectively, while approximately 99.9% for the GLS, CN and BE uniform time step schemes. As shown in Fig. 7, this accurate latent heat balance performance of the proposed method results in an oscillating time-step history profile. Furthermore, the proposed method has the smaller CPU time (performed by ASUS A8FM PC with an Intel Core 2 1.83 (MHz) CPU and 1024 MB RAM) than those uniform time step methods.

5. Conclusions

This study has presented an adaptive time-step control scheme based on a modified LTE technique. In the approach presented in this study, the LTE-based time-step evaluation procedure is applied not only after a convergent temperature field is obtained at each time step, but also during the nonlinear iterations performed at each time step whenever a convergence problem is encountered. This would make it possible for the implicit method to solve the unstably convergent problems of solidification processes. The various performances of the proposed approach have been demonstrated via the simulation of the 1-D and 2-D solidification problems and compared with those of the GLS, CN, BE adaptive time step methods, and the corresponding uniform time step methods. The performance of the proposed approach has also been demonstrated using fully-implicit and semi-implicit schemes. In general, the results have shown that the proposed approach has a high numerical accuracy (as evaluated by comparing the computed value of the total latent heat released with the exact solution), a high computational efficiency (as indicated by a low CPU time and a low total number of time steps in the simulation procedure). Moreover, since the time steps predicted by the proposed method are based on the local temperature, it is expected that this method can provides a flexible reference tool for the researchers while they investigate other transient phenomena of a casting or solidification process, such as velocity and concentration fields, not limited in the isothermal process.

References

[1] W. Kurz, D.J. Fisher, Fundamentals of Solidification, Trans Tech Publications, Switzerland, 1998.
[2] A.J. Dalhuijsen, A. Segal, Comparison of finite element techniques for solidification problems, Int. J. Numer. Methods Eng. 23 (1986) 1807–1829.
[3] D. Poirier, M. Salcudean, On numerical methods used in mathematical modeling of phase change in liquid metals, J. Heat Transf.—Trans. ASME 110 (1988) 562–570.
[4] V.R. Voller, C.R. Swaminathan, Fixed grid techniques for phase change problems: a review, Int. J. Numer. Methods Eng. 30 (1990) 875–898.
[5] H. Hu, S.A. Argyropoulos, Mathematical modeling of solidification and melting: a review, Model. Simul. Mater. Sci. Eng. 4 (1996) 371–396.
[6] R.W. Lewis, K. Ravindran, Finite element simulation of metal casting, Int. J. Numer. Methods Eng. 47 (2000) 29–59.
[7] K.K. Tamma, R.R. Namburu, Recent advances, trends and new perspectives via enthalpy-based finite element formulations for applications to solidification problems, Int. J. Numer. Methods Eng. 30 (1990) 803–820.
[8] T. Ouyang, K.K. Tamma, Finite element simulations involving simultaneous multiple interface fronts in phase change problems, Int. J. Heat Mass Transf. 39 (1996) 1711–1718.
[9] R.R. Namburu, K.K. Tamma, Effective modeling/analysis of isothermal phase change problems with emphasis on representative enthalpy architectures and finite elements, Int. J. Heat Mass Transf. 36 (1993) 4493–4497.
[10] Y. Mei, R.V. Mohan, K.K. Tamma, Evaluation and applicability of a new explicit time integral methodology for transient thermal problems-finite volume formulations, Numer Heat Transfer B—Fundam. 26 (1994) 313–333.
[11] J. Douglas, T.M. Gallie, On the numerical integration of a parabolic differential equation subject to a moving boundary condition, Duke Math. J. 22 (1995) 557–571.
[12] J.S. Goodling, M.S. Khader, Inward solidification with radiation-convection boundary condition, J. Heat Transfer—Trans. ASME 96 (1974) 114–115.
[13] R.S. Gupta, D. Kumar, A modified variable time step method for one-dimensional Stefan problem, Comput. Meth. Appl. Mech. Eng. 23 (1980) 101–109.
[14] R.S. Gupta, D. Kumar, Variable time step methods for one-dimensional Stefan problem with mixed boundary condition, Int. J. Heat Mass Transfer 24 (1981) 251–259.
[15] T. Ouyang, K.K. Tamma, On adaptive time stepping approaches for thermal solidification processes, Int. J. Numer. Meth. Heat Fluid Flow 6 (1996) 37–50.
[16] P.M. Gresho, R.L. Lee, R.L. Sani, On the time dependent solution of the incompressible Navier–Stokes equations in two and three dimensions, in: Recent Advance in Numerical Methods in Fluids, Pineridge Press, Swansea, 1980.
[17] FIDAP Theory Manual, Fluent Inc., New Hampshire, 1998.
[18] H.C. Peng, L.S. Chao, Adaptive time stepping control for thermal solidification processes by utilizing the extreme of local time truncation error, in: C.K. Chao, C.Y. Lin (Eds.), Proceedings of 7th International Congress on Thermal Stresses, National Taiwan University of Science and Technology, Taipei, Taiwan, 2007, pp. 619–622.
[19] S.V. Patankar, Numerical Heat Transfer and Fluid Flow, Hemisphere Publishing Corporation, New York, 1980.
[20] J. Stefan, Über die Theorie der Eisbildung, insbesondere über die Eisbildung in Polarmaere, Annalen der Physik and Chemie 42 (1891) 269–286.
[21] K.A. Rathjen, L.M. Jiji, Heat conduction with melting or freezing in a corner, J. Heat Transfer—Trans. ASME 93 (1971) 101–109.